Cellulose
https://doi.org/10.1007/s10570-024-06149-4

ORIGINAL RESEARCH

Chitosan coatings reinforced with cellulose crystals and oregano essential oil as antimicrobial protection against the microbiological contamination of stone sculptures

Nádia C. Silva · Ana Raquel Madureira · Manuela Pintado · Patrícia R. Moreira

Received: 25 March 2024 / Accepted: 26 August 2024

Abstract The proliferation of microorganisms in outdoor stone sculptures and cultural objects can damage the structure and aesthetics of the materials through biodeterioration mechanisms. Biocides and synthetic products are often used to prevent this phenomenon, despite their negative impact on the environment and human health. Less toxic alternatives with reduced environmental impact can be an option for the preventive conservation of stone sculptures to reduce the environmental impact. In this work, chitosan formulations reinforced with two types of cellulose crystals (microcrystalline cellulose (MCC) or cellulose nanocrystals (CNCs)) and with or without citric acid and sodium tripolyphosphate were prepared. The films obtained with these formulations showed low solubility, and those only containing MCC or CNCs had the lowest wettability. The formulation containing 2% (w/v) MCC was selected for further analysis and supplemented with oregano essential oil (OEO) at 1% (v/v) and 2% (v/v), exhibiting low solubility, swelling and wettability when polymerised in film form. Inoculation of the films with *Staphylococcus aureus*, *Bacillus cereus*, *Pseudomonas aeruginosa* and *Rhodotorula* spp. resulted in total or partial inhibition of their growth, as well as a 60–100% reduction in *Penicillium chrysogenum* growth, depending on the concentration of OEO. The formulation with 2% (v/v) OEO was applied to samples of granite, marble and limestone, forming a protective, yet irregular coating on their surfaces. The wettability of the stones' surfaces was reduced without becoming completely water-repellent and the coating did not cause visible colour changes.

Keywords Chitosan · Essential oil · Microcrystalline cellulose · Cellulose nanocrystals · Stone · Cultural heritage

Introduction

Stone heritage, such as buildings, monuments and sculptures, is exposed to a variety of agents that contribute to its deterioration over time. Climatic factors, such as rain, wind and solar radiation, together with atmospheric pollution, contribute significantly to chemical and physical changes in stone materials, ultimately accelerating their decay (Herrera

Supplementary Information The online version contains supplementary material available at https://doi.org/10.1007/s10570-024-06149-4.

N. C. Silva · A. R. Madureira · M. Pintado · P. R. Moreira
Universidade Católica Portuguesa, CBQF - Centro de Biotecnologia e Química Fina – Laboratório Associado, Escola Superior de Biotecnologia, Rua Diogo Botelho 1327, 4169-005 Porto, Portugal

P. R. Moreira (✉)
Universidade Católica Portuguesa, CITAR - Centro de Investigação Em Ciência E Tecnologia das Artes, Escola das Artes, Rua Diogo Botelho 1327, 4169-005 Porto, Portugal
e-mail: prmoreira@ucp.pt

Published online: 01 October 2024

and Videla 2009; Dakal and Cameotra 2012; Gadd 2017). In addition, the deterioration of stone heritage is enhanced by the growth and metabolic activity of microorganisms that colonise the surfaces and the inner strata of stone materials (Herrera and Videla 2009; Gadd 2017; Negi and Sarethy 2019; Liu et al. 2020). As the influence of atmospheric factors is not controllable when monuments and artworks are displayed outdoors, the colonisation and proliferation of biological agents in stone are often managed with biocides and synthetic polymer coatings (Ranalli et al. 2009; Sierra-Fernandez et al. 2017). However, these types of products can be toxic to the environment and human health or be abrasive to the stone structure itself (Ranalli et al. 2009; Sasso et al. 2016; Sierra-Fernandez et al. 2017). The development of less toxic, more compatible and environmentally friendly coatings is a potential resource to prevent microbial degradation of stone heritage and be an alternative to the biocides currently used (Ocak et al. 2009; Kakakhel et al. 2019; Kaplan et al. 2019). Additionally, the reversibility of treatments in stone heritage is a desirable feature, so the design of protective coatings that are not permanent and can be removed or reapplied as required should be considered (Ocak et al. 2009; Kaplan et al. 2019). Such characteristics are found in biodegradable polymers and can be explored in the context of preventive conservation of cultural heritage.

Chitosan is one of the most abundant polymers in nature and can be obtained from chitin as a by-product of seafood waste, since chitin is a major component of the exoskeleton of crustaceans (Rinaudo 2006; Bakshi et al. 2020; Mathew et al. 2020). Chitosan is used to produce films and coatings for applications in several fields, including biomedicine and the food industry, due to its non-toxicity and good biocompatibility, biodegradability and antimicrobial activity against several groups of microorganisms (Bakshi et al. 2020; Haghighi et al. 2020; Kumar et al. 2020). However, chitosan films and coatings are affected by water and moisture, which limits their applicability in some circumstances (Ocak et al. 2009; Abdul Khalil et al. 2019). In the case of stone art objects, coatings applied to their surfaces must be able to withstand the presence of water after polymerisation and retain their overall structure (Silva et al. 2024). This becomes even more relevant for outdoor stone artworks and monuments that are exposed to atmospheric conditions such as rain and high humidity.

Nevertheless, chitosan-based formulations can be reinforced with various cross-linkers, fillers and additives to improve the properties of the polymer matrix. For example, microcrystalline cellulose (MCC) and cellulose nanocrystals (CNCs), which are extracted from plant and wood residues by mechanical and chemical treatments on cellulose, have been used as reinforcing materials in biopolymer formulations, forming compact networks that improve the mechanical and barrier properties of the composites (Jahed et al. 2017; Franco et al. 2020; Jung et al. 2020; Ponnusamy et al. 2022). Similarly, sodium tripolyphosphate (TPP) and citric acid have been used as cross-linking agents in chitosan films and membranes to improve their functional features (Lusiana et al. 2017; Tomaz et al. 2018; C. Wu et al. 2019a, b; Guerrero et al. 2019; H. Wu et al. 2019a, b; Silva et al. 2024). Other additives can also be incorporated into chitosan composites to enhance specific properties, as is the case with essential oils due to their antimicrobial capacity (Wu et al. 2014; Chen et al. 2020).

Thus, the aim of this work was to develop a low-toxicity formulation to be applied as a biodegradable antimicrobial protective coating on stone surfaces of culturally relevant objects, such as urban outdoor sculptures. To this purpose, a screening of sixteen chitosan formulations reinforced with MCC and CNCs, with or without citric acid and TPP, was carried out in order to test different types and degrees of cross-linking and reinforcing agents and choose the formulation with the most suitable properties for the desired application. The selected formulation was then supplemented with oregano essential oil (OEO) and evaluated for its physicochemical properties and antimicrobial capacity against microorganisms that commonly comprise stone microbiomes. The applicability of the coating was tested on granite, marble and limestone in order to assess possible changes in the wettability and colour of the stone surfaces.

Experimental

Medium molecular weight chitosan (190,000–310,000 Da) with 75–85% deacetylation, citric acid monohydrate, TPP and TWEEN® 80 were obtained from Sigma-Aldrich (USA). MCC (Avicel®

PH-101) was purchased from Sigma-Aldrich (USA) and CNCs (CelluForce NCC®) was acquired from CelluForce (Canada). Glycerol and glacial acetic acid were purchased from Merck (Germany). OEO (from *Origanum vulgare*) was obtained from Assemis (Portugal). Müller-Hinton (MH) broth and agar culture media, as well as potato dextrose agar (PDA), were acquired from BIOKAR Diagnostics (France), while potato dextrose broth (PDB) was purchased from Laboratorios Conda (Spain). Bacteriological peptone was obtained from HiMedia® Laboratories (India). Slabs of granite, limestone and marble were acquired from Mármores e Granitos Felisberto, Lda (Portugal).

Preparation of chitosan-based formulations reinforced with MCC or CNCs

The preparation of the chitosan-based coatings was carried out according to Silva et al. (2024) with modifications. Chitosan (1% (w/v)) was added to an aqueous solution of acetic acid (1% (v/v)) and stirred continuously until complete dissolution. Glycerol (1% (w/v)) was dissolved in 15 mL of the previously prepared chitosan solution at 600 rpm for 2 h; in some formulations, citric acid (1% (w/v)) was added simultaneously with glycerol. MCC or CNCs at 1% (w/v) or 2% (w/v) were added to the previous mixture and stirred at 700 rpm for 1 h to resuspend the cellulose crystals, after which the mixtures were sonicated with an ultrasonic processor at 70% amplitude for 2 min (SONICS Vibra-Cell™ VCX-130, Sonics & Materials, USA). For some formulations, 6 mL of an aqueous solution of TPP at 0.25% (w/v) was added dropwise to the previous mixtures using a syringe pump (KDS 100 Legacy, KD Scientific, USA) at a flow rate of 250 µL min^{-1} under stirring (1,000 rpm). The coating-forming solutions were stirred at 1,000 rpm for 10 min to complete homogenisation, transferred to plastic Petri dishes (6 mL in 52 mm diameter dishes) and left at room temperature for 72 h to evaporate the solvents and polymerise the solutions into solid films. The formulations were labelled as shown in Table 1.

Table 1 Concentration of the reagents used to prepare the chitosan/MCC- and chitosan/CNC-based formulations

Sample	Concentration (%)				
	MCC	CNC	CA	TPP	OEO
1-MCC-CA	1	0	1	0	0
2-MCC-CA	2	0	1	0	0
1-MCC-CA-TPP	1	0	1	0.25	0
2-MCC-CA-TPP	2	0	1	0.25	0
1-MCC	1	0	0	0	0
2-MCC	2	0	0	0	0
1-MCC-TPP	1	0	0	0.25	0
2-MCC-TPP	2	0	0	0.25	0
1-CNC-CA	0	1	1	0	0
2-CNC-CA	0	2	1	0	0
1-CNC-CA-TPP	0	1	1	0.25	0
2-CNC-CA-TPP	0	2	1	0.25	0
1-CNC	0	1	0	0	0
2-CNC	0	2	0	0	0
1-CNC-TPP	0	1	0	0.25	0
2-CNC-TPP	0	2	0	0.25	0
2-MCC-OEO-1	2	0	0	0	1
2-MCC-OEO-2	2	0	0	0	2

The concentrations of chitosan, acetic acid and glycerol were fixed at 1% for all formulations. CA: citric acid; CNC: cellulose nanocrystals; MCC: microcrystalline cellulose; OEO: oregano essential oil; TPP: sodium tripolyphosphate

Characterisation of chitosan-based formulations reinforced with MCC or CNCs

Assessment of water solubility

Solubility assays of the chitosan-based formulations with MCC or CNCs were performed in triplicate according to Silva et al. (2024). Briefly, the films polymerised as described above were placed on dried glass Petri dishes and put in an oven at 105 °C. The films were dried and weighed until a constant weight was reached, after which 35 mL of deionised water was added to the Petri dishes to submerge the films for 24 h. After removing the water, the films were dried at 105 °C for 24 h and weighed to determine the final dry weight. All measurements were carried out using an analytical balance (ACJ 120-4 M, Kern & Sohn, Germany). The percentage of solubility of the films was calculated according to the same authors.

Water contact angle measurements

Water contact angle (WCA) measurements were done by the sessile drop technique (Laplace-Young method) with a tensiometer (Attension Theta, Biolin Scientific, Sweden) in order to evaluate the wettability properties of the films (Silva et al. 2024). Drops (3 µL) of deionised water were placed on each film at three different points and the WCA values were registered for 1 min. The mean WCA of each film was calculated using the values registered 3 s after the start of the experiments to allow the water droplets to stabilise. The experiment was repeated by testing three specimens of each type of film and calculating the mean WCA values.

Preparation of chitosan-based formulations reinforced with MCC and OEO

Chitosan (1% (w/v)) was dissolved in an aqueous solution of acetic acid (1% (v/v)). Glycerol at 1% (w/v) was added and stirred at 600 rpm for 2 h, after which MCC at 2% (w/v) was hydrated in the previous solution with constant stirring at 700 rpm for 1 h. The mixture (2-MCC) was sonicated for 2 min (70% amplitude) and OEO at 1% or 2% (v/v) was added and stirred at 700 rpm for 1 h. The resulting coating-forming solutions (Table 1: 2-MCC-OEO-1 and 2-MCC-OEO-2) were poured into plastic Petri dishes (6 mL in 52 mm diameter dishes) and left at room temperature for 72 h to polymerise into solid films and carry out their characterisation.

Characterisation of chitosan-based formulations reinforced with MCC and OEO

Fourier transformed infrared spectroscopy

Fourier Transformed Infrared (FTIR) spectra of pure OEO and the 2-MCC, 2-MCC-OEO-1 and 2-MCC-OEO-2 films were obtained using a PerkinElmer Precisely Spectrum 100 FTIR spectrometer (Waltham, USA) connected to an attenuated total reflectance accessory (PIKE MIRacle™, PIKE Technologies, USA) with a diamond crystal plate. Eight scans were made for each sample at 4 cm^{-1} resolution between 4,000 and 550 cm^{-1} (Silva et al. 2024).

Assessment of water solubility and swelling

The solubility of the 2-MCC-OEO-1 and 2-MCC-OEO-2 films was determined following the same protocol detailed above. The swelling tests were performed as reported by Silva et al. (2024). Briefly, the films were placed on dried glass Petri dishes and put in an oven at 105 °C. The films were dried and weighed until reaching a constant weight, after which they were submerged in 35 mL of deionised water for 24 h. After the water was removed, the excess water was absorbed with filter paper and the films were weighed to obtain their wet weight. The percentage of swelling was calculated according to the same authors.

Water contact angle measurements

The wettability of the 2-MCC-OEO-1 and 2-MCC-OEO-2 films was evaluated following the protocol described above.

Antimicrobial activity assays

Antimicrobial activity assays were executed following the same protocol and microorganisms described by Silva and co-authors (2024), as representatives of taxa that can be found in stone heritage microbiomes and be involved in alterations of its structure and aesthetics (Silva et al. 2024). *Staphylococcus aureus* (ATCC® 25,923™), *Bacillus cereus* (NCTC 2599) and *Pseudomonas aeruginosa* (ATCC® 27,853™) were grown in MH broth at 37 °C, while *Rhodotorula* spp. (CBS 10577) and *Penicillium chrysogenum* (ATCC® 10,106™) were grown in PDB at 22 °C and 25 °C, respectively. Before the assays, calibration curves of optical density (OD) at 600 nm versus concentrations of *S. aureus*, *B. cereus*, *Pseudomonas aeruginosa* and *Rhodotorula* spp. cells were generated following the protocol of Silva et al. (2024). A calibration curve of OD versus concentration of *Penicillium chrysogenum* spores was also produced according to the same authors. These calibration curves were plotted in order to adjust the microbial inocula to the desired concentrations of viable cells and spores for the antimicrobial activity assays.

Evaluation of the inhibition of viable microbial cells

Viable cell count assays for *S. aureus*, *B. cereus*, *Pseudomonas aeruginosa* and *Rhodotorula* spp. were performed according to Silva et al. (2024). Briefly, suspensions of *S. aureus* and *P. aeruginosa* were grown in MH broth at 37 °C for 16 h, while suspensions of *B. cereus* were prepared using the same culture medium and incubated at 30 °C for 16 h. Cell suspensions of *Rhodotorula* spp. were prepared in PDB and incubated at 22 °C for 65 h. The suspensions were then diluted in peptone water (1 g L^{-1}) to a concentration of 5×10^6 colony forming units (CFUs) mL^{-1}, using a spectrophotometer (UV mini-1240, Shimadzu, Japan) and the calibration curves reported above. The 2-MCC, 2-MCC-OEO-1 and 2-MCC-OEO-2 films were cut into small discs (1 cm^2), sterilised under UV-C light for 10 min on each side and placed in sterile tubes. Each tube was filled with 200 µL of inoculum and 200 µL of MH broth or PDB, depending on the microorganism being tested. Tubes without film discs were filled in the same manner and used as positive controls for the growth of the microbial strains. Tubes with film discs loaded with 400 µL of MH broth or PDB were used as negative controls. The tubes were incubated at 37 °C (*S. aureus* and *P. aeruginosa*), 30 °C (*B. cereus*) or 22 °C (*Rhodotorula* spp.) and 200 µL were aseptically collected from each tube at 0 h, 3 h, 6 h and 24 h (for the bacteria) or 0 h, 3 h, 6 h, 24 h, 48 h, 55 h and 78 h (for the yeast). The aliquots were transferred to sterile tubes containing 1.8 mL of peptone water (1 g L^{-1}) and serially diluted (1:10) in the same solution. Twenty µL of each dilution was plated in triplicate on MH agar (*S. aureus*, *B. cereus* and *P. aeruginosa*) or PDA (*Rhodotorula* spp.) plates by the drop plate technique. The plates were incubated for 24 h (bacteria) or 65 h (yeast) at the temperature appropriate for each strain, after which the number of CFUs was counted and the concentrations of viable cells and logarithmic reduction in microbial growth were calculated.

Evaluation of the inhibition of fungal spore germination

The ability of the 2-MCC, 2-MCC-OEO-1 and 2-MCC-OEO-2 films to inhibit the germination of *Penicillium chrysogenum* spores and fungal growth was evaluated according to Silva et al. (2024). A suspension of spores was prepared by adding a solution of TWEEN® 80 (1% (w/v)) in peptone water (1 g L^{-1}) to PDA plates inoculated with *P. chrysogenum* and transferring the spores to a sterile tube. The concentration of spores was adjusted to 2.5×10^6 spores mL^{-1} using a spectrophotometer (UV mini-1240, Shimadzu, Japan) and the calibration curve previously calculated as described above. The films, previously cut into discs (1 cm^2) and sterilised under UV-C light for 10 min on each side, were transferred to PDA plates and 10 µL of the spore suspension was placed on each film. Positive controls were performed in the same way, but using sterile filter paper discs; negative controls were prepared with PDA plates containing film discs without spores. The agar plates were incubated at 25 °C and the diameter of the colonies was recorded after 4 days to calculate the percentage of inhibition of fungal growth (Silva et al. 2024). The experiment was conducted in triplicate.

Evaluation of the 2-MCC-OEO-2 formulation applied to stone slabs

The formulation containing 2% OEO (2-MCC-OEO-2) was applied to samples of granite, limestone and marble (which had been washed beforehand with deionised water) and allowed to settle at room temperature until fully dried, according to the protocols described in the following sections.

Scanning electron microscopy

Slabs of granite, limestone and marble (1 × 1 × 1 cm) were coated with 25 µL of 2-MCC-OEO-2, using micropipette tips to spread the solution over the upper surfaces, and allowed to dry completely (Silva et al. 2024). The stones were mounted on a sample holder and observed with a Phenom Pro scanning electron microscope (Thermo Fisher Scientific, USA), equipped with a backscattered electron detector, at room temperature and an accelerating voltage of 10 kV.

Fourier transformed infrared spectroscopy

The upper surfaces of granite, limestone and marble slabs (4 × 4 × 1 cm) were coated with 400 µL of 2-MCC-OEO-2, using micropipette tips to spread the

solution (Silva et al. 2024), and analysed by FTIR spectroscopy using the same equipment and methodology reported above.

Water contact angle assessment

Four hundred µL of 2-MCC-OEO-2 were spread over the upper surfaces of granite, limestone and marble samples (4×4×1 cm) using micropipette tips (Silva et al. 2024). WCAs of the coated stones were determined following the protocol and equipment described above. The experiments were conducted in triplicate.

Colour measurements

The colour changes of granite, limestone and marble samples (4×4×1 cm) before and after coating with 2-MCC-OEO-2 were evaluated by colourimetric measurements using a CM-700d Chroma Meter (Konica Minolta, Japan) (Silva et al. 2024). Firstly, CIELab L* a* b* values were recorded over the upper surfaces of uncoated slabs. Then, 400 µL of 2-MCC-OEO-2 were applied to the same stones, using micropipette tips or a brush to spread the formulation over the upper surfaces, and allowed to dry for 24 h. Twenty measurements were taken for each specimen before and after coating and the mean values of the L* a* b* coordinates were calculated; the protocol was repeated in triplicate and the total colour difference (ΔE^*_{ab}) of the stone surfaces before and after coating was calculated according to Silva et al. (2024).

Statistical analysis

Statistical analysis was executed with IBM SPSS® Statistics v28 software (IBM, USA). The normal distribution of the data was confirmed by the Shapiro–Wilk test. Statistically significant differences among the chitosan/MCC- and chitosan/CNC-based formulations, as well as differences among the formulations with and without OEO, were calculated by one-way analysis of variance (ANOVA) with the Tukey B post-hoc test. Growth inhibition of *Penicillium chrysogenum* when in contact with each film and the positive control was evaluated by independent samples t-tests. The WCAs of uncoated and 2-MCC-OEO-2-coated stone samples, as well as the colour differences of the samples according to the method of coating application (micropipette or brush), were evaluated by independent samples t-tests.

Results and discussion

Aspect, solubility and wettability of chitosan-based formulations reinforced with MCC or CNCs

The films resulting from the polymerisation of the chitosan-based formulations with MCC or CNCs were malleable and had a uniform aspect to the naked eye, as shown in Fig. 1.

At the end of the solubility assays (24 h), the films were visually intact after continuous immersion in water. Similar results were reported by Ponnusamy et al. (2022), who observed that chitosan films cross-linked with cellulose nanofibrils showed no damage after immersion in deionised water. The authors suggested that the establishment of hydrogen bonds between chitosan and cellulose nanofibrils provided a reinforced matrix and reduced the number of hydroxyl groups capable of reacting with water molecules (Ponnusamy et al. 2022).

The chitosan/MCC- and chitosan/CNC-based films had solubility percentages below 30% (Fig. 2).

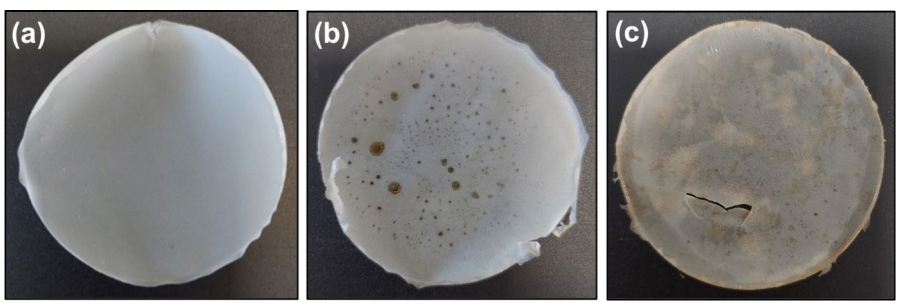

Fig. 1 Example of **a** a chitosan-based film reinforced with cellulose crystals (2-MCC formulation), and of chitosan/MCC-based films reinforced with **b** 1% (2-MCC-OEO-1) and **c** 2% (2-MCC-OEO-2) OEO. MCC: microcrystalline cellulose; OEO: oregano essential oil

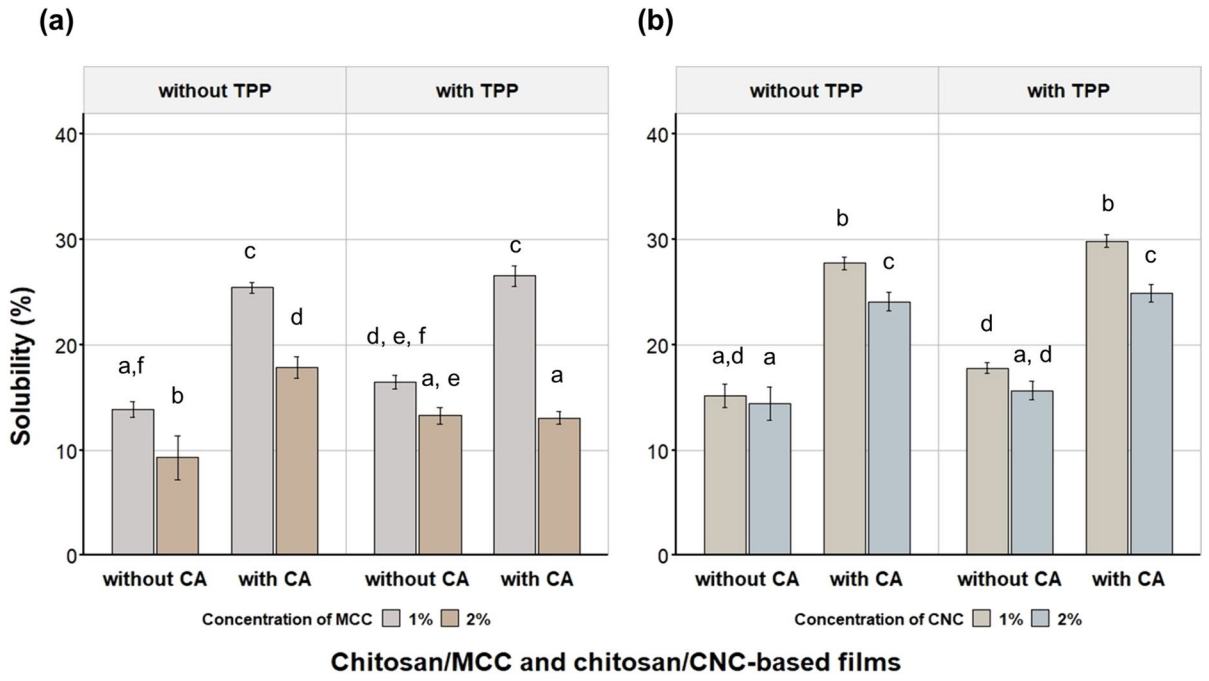

Fig. 2 Solubility of **a** chitosan/MCC- and **b** chitosan/CNC-based films. The values represent the mean ± standard deviation (n = 3). Statistically significant differences are represented by different letters (one-way ANOVA with Tukey B post-hoc test; α = 0.01). CA: citric acid; CNC: cellulose nanocrystals; MCC: microcrystalline cellulose; TPP: sodium tripolyphosphate

Overall, the formulations containing 2% MCC formed significantly less soluble films ($p < 0.01$) than the equivalent formulations prepared with a lower concentration (1%) of MCC (Fig. 2a). In the formulations containing either 1% or 2% MCC, the addition of citric acid resulted in a significant increase in the solubility of the films ($p < 0.01$). When TPP was added to the formulations containing citric acid (1- and 2-MCC-CA versus 1- and 2-MCC-CA-TPP), the solubility of the films with 1% MCC was maintained, but those prepared with 2% MCC became significantly less soluble (from 17.86 ± 1.03 to 13.07 ± 0.60%; $p < 0.01$). When TPP was added to the formulations without citric acid, the percentage of solubility increased significantly ($p < 0.01$) only for the films with 2% MCC (2-MCC: 9.27 ± 2.11% versus 2-MCC-TPP: 13.27 ± 0.81%). The same trend was observed for the formulations developed with CNCs (Fig. 2b). Overall, the films with 2% CNCs were equally or significantly less soluble ($p < 0.01$) than those with a lower concentration of CNCs. Like the MCC films, the CNCs films without citric acid were significantly less soluble (ranging from 15.14 ± 1.12 to 17.77 ± 0.52%; $p < 0.01$) than the same films with citric acid (ranging from 24.09 ± 0.89 to 29.85 ± 0.58%). The addition of TPP to the CNC formulations without citric acid did not affect the solubility properties of the films. However, when TPP was incorporated into the formulations already containing citric acid, the solubility percentages of the films increased significantly (from 1-CNC: 15.14 ± 1.12 to 1-CNC-CA-TPP:29.85 ± 0.58% and from 2-CNC: 14.45 ± 1.59 to 1-CNC-CA-TPP: 24.91 ± 0.84%; $p < 0.01$); this was independent of the concentration of CNCs. Additionally, considering both types of cellulose crystals, 2-MCC was significantly less soluble than all the other formulations ($p < 0.01$).

The solubility of the films varied with the concentration of cellulose crystals, with higher concentrations culminating in either equal or significantly less soluble membranes. This suggests an increase in intermolecular interactions between chitosan and either MCC or CNCs at higher concentrations and the formation of more compact networks, restricting the number of available reactive groups and water interactions and uptake (Franco et al. 2020; Ponnusamy

et al. 2022). The introduction of citric acid and TPP as additional crosslinkers was also tested to assess the changes in film solubility. The presence of TPP or citric acid either maintained or slightly increased the solubility of the films when compared to the formulations containing only MCC or CNCs. Incorporating citric acid and TPP possibly increased the number of reactive groups. Consequently, the excess of hydroxyl and carboxyl groups may have enhanced the interactions with water molecules and contributed to the slight increase in film solubility (Wu et al. 2019a, b; Ponnusamy et al. 2022). Therefore, MCC or CNCs alone were sufficient to ensure solid and stable chitosan matrices, with low percentages of solubility (< ca. 15%).

The wettability assays were carried out by measuring the contact angles formed between water droplets and the surfaces of the films (Fig. 3). Mean WCAs > 50° were recorded for the films containing MCC (Fig. 3a). The highest WCA values were registered when these formulations did not contain citric acid; in particular, mean WCAs > 90° were recorded for 1-MCC-TPP and 2-MCC. On the contrary, the addition of citric acid maintained (1-MCC versus 1-MCC-CA) or significantly reduced (all other formulations; $p < 0.01$) the WCAs of the films, especially when combined with TPP. No statistically significant differences were observed regarding the concentration of MCC ($p > 0.01$). The films containing CNCs (Fig. 3b) showed wettability characteristics similar to those with MCC. Films with WCAs < 90° were produced from most formulations, particularly those containing TPP (ranging from 41.92 ± 2.40° to 48.64 ± 2.58°). A slightly higher mean WCA was recorded for the formulation with CNCs and citric acid (ca. 60°). However, only 2-CNC resulted in a film with an average WCA > 90°. Additionally, with the exception of 1- and 2-CNC, the films prepared with CNCs exhibited equal or significantly greater wettability ($p < 0.01$) than those containing MCC. Overall, the addition of TPP and citric acid seems to have led to a more pronounced effect on the wettability properties of the films containing CNCs than on those with MCC.

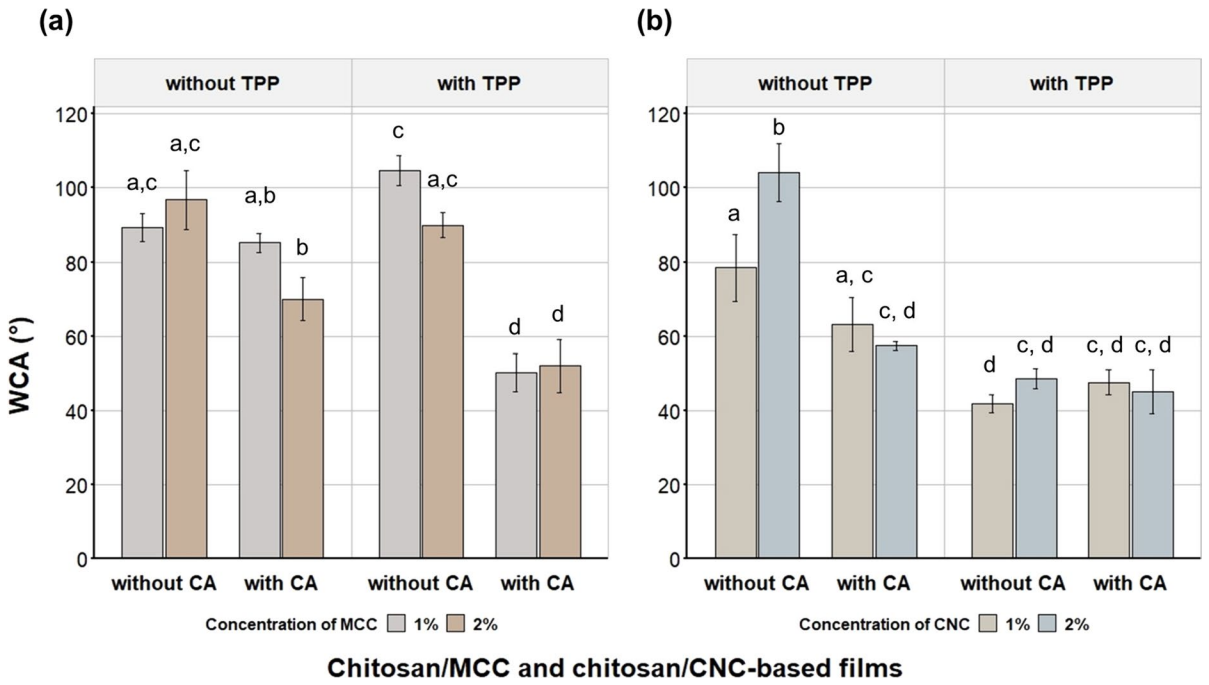

Fig. 3 Water contact angle of **a** chitosan/MCC- and **b** chitosan/CNC-based films. The values represent the mean ± standard deviation (n = 3). Statistically significant differences are represented by different letters (one-way ANOVA with Tukey B post-hoc test; α = 0.01). CA: citric acid; CNC: cellulose nanocrystals; MCC: microcrystalline cellulose; TPP: sodium tripolyphosphate; WCA: water contact angle

The wettability assays supported the solubility results reported above. Most films showed high wettability, with WCAs < 90º, especially those containing citric acid and TPP. This arises from the excessive availability of free polar groups (Guerrero et al. 2019; Ponnusamy et al. 2022). Nevertheless, some films showed WCAs > 90° or close to this threshold of water-repellence. This was the case for the MCC formulations prepared without citric acid (with or without TPP) and with citric acid and no TPP, as well as those that contained only CNCs.

In summary, both MCC and CNCs cross-linked effectively with chitosan, resulting in poorly soluble films after polymerisation of the coating-forming solutions. The films were malleable and remained visually intact for up to 24 h of immersion in water. The formulations containing MCC or CNCs (without citric acid or TPP) originated films with low wettability, above or near the water-repellence threshold. Overall, the presence of TPP and/or citric acid did not improve the solubility and wettability properties of the films, possibly due to the excessive availability of reactive groups. Therefore, and considering the intended application, 2-MCC was selected for further analysis, since the resulting films were simultaneously significantly less soluble than the others and showed WCAs above the water-repellence threshold (WCA > 90°).

Characterisation of chitosan-based formulations reinforced with MCC and OEO

The 2-MCC formulation was further supplemented with OEO (see Table 1), resulting in solutions with final pH values of ca. 3.8. After polymerisation, the films (Fig. 1b and c) were characterised concerning their physicochemical properties and antimicrobial capacity against microorganisms associated with stone microbiomes.

Physicochemical characterisation

Fourier transformed infrared spectroscopy

Regarding the presence of functional groups, FTIR spectra (Fig. 4a) showed absorption bands in the 3,500–3,200 cm^{-1} and 2,900–2,800 cm^{-1} regions, which can be attributed to O−H and N−H stretching vibrations and vibrations in the C−H bonds, respectively (Bagheri et al. 2015; Gierszewska and Ostrowska-Czubenko 2016; Guerrero et al. 2019; Chen et al. 2020; Pavinatto et al. 2020; Sogut and Cakmak 2020; Silva et al. 2024). These absorption bands are typical of chemical groups present in both chitosan and MCC and have been associated in other studies with effective cross-linking between the two compounds (Marín-Silva et al. 2019; Chen et al. 2020; Sogut and Cakmak 2020). Specifically, a shift in the absorption peak of MCC from 3,335 to 3,276 cm^{-1} was detected after the reagent was incorporated with chitosan in the 2-MCC formulation; a similar wavenumber shift occurred from 2,896 to 2,885 cm^{-1}. Additionally, some peaks (1,315 cm^{-1} and 1,053 cm^{-1}) were observed for pure MCC that were no longer visible after its incorporation into the chitosan-based solution. These changes suggest the formation of new bonds between the two compounds. Similar observations were made by Marín-Silva et al. (2019), who ascribed a shift at 3,500–3,200 cm^{-1} to possible bonding between −OH groups from cellulose and available $-NH_2$ groups from chitosan. A shift at 2,900–2,800 cm^{-1} after the addition of MCC was previously noticed in FTIR spectra of cellulose materials in the presence of chitosan, which was attributed to C−H vibrations common in polysaccharide spectra (Marín-Silva et al. 2019).

Absorption bands between 1,650 and 1,500 cm^{-1} were also identified, which have been associated with the amide groups of chitosan in other studies. Specifically, the band at ca. 1,640 cm^{-1} was identified as the amide I band associated with C=O stretching vibrations, whereas the absorption band in the 1,560–1,550 cm^{-1} region was attributed to the amide II band of C−N stretching and N−H bending vibrations (Sacco et al. 2014; Liu et al. 2016; Pavinatto et al. 2020; Silva et al. 2024). Similarly, bands related to the chitosan ring structures, namely vibrations of $C-CH_3$ or C−O bonds, were also detected at 1,408–1,422 cm^{-1} (Sacco et al. 2014; Bagheri et al. 2015). The peak at ca. 1,160 cm^{-1} could be related to C−O−C vibrations, as well as the peak at 1,030 cm^{-1}, which has been assigned in previous studies to the C−O bonds found in both chitosan and cellulosic materials (Guerrero et al. 2019; Marín-Silva et al. 2019; Chen et al. 2020; Sogut and Cakmak 2020; Silva et al. 2024).

The addition of OEO to the formulation was indicated by wavenumber shifts and an increase in

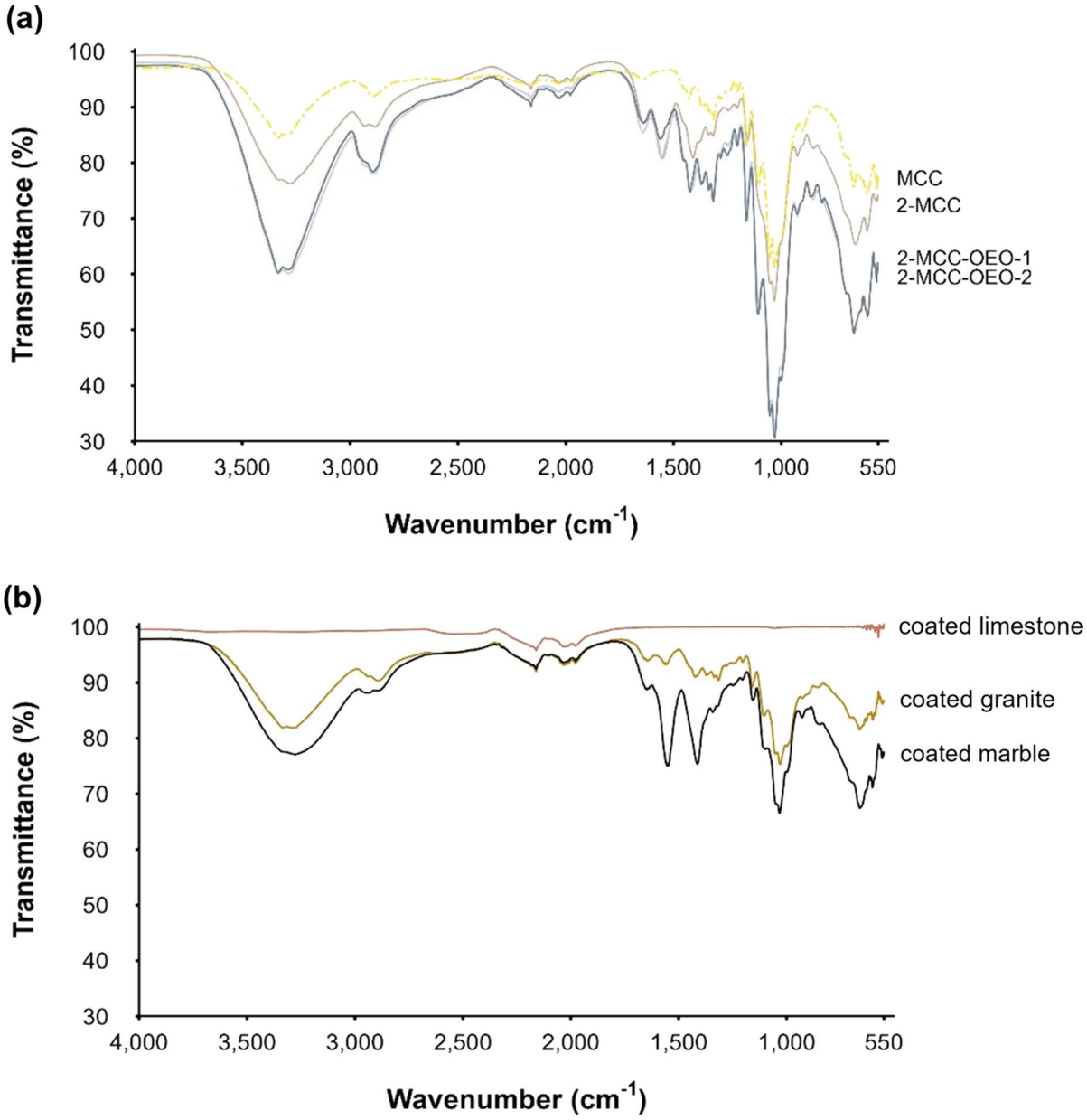

Fig. 4 FTIR spectra of **a** MCC and chitosan/MCC-based films (2-MCC), including those reinforced with 1% (2-MCC-OEO-1) and 2% (2-MCC-OEO-2) OEO, and (b) 2-MCCOEO-2 coated granite, marble and limestone. MCC: microcrystalline cellulose; OEO: oregano essential oil

the intensity of some absorption peaks (Fig. 4 a). This is the case of the peaks at 3,500–3,200 cm^{-1} and 2,900–2,800 cm^{-1} assigned to O−H, N−H, C−H and C−O bonds (Bagheri et al. 2015; Gierszewska and Ostrowska-Czubenko 2016; Guerrero et al. 2019; Chen et al. 2020; Pavinatto et al. 2020; Sogut and Cakmak 2020; Silva et al. 2024). Chen et al. (2020) reported an increase in peak intensity at 2,921–2,863 cm^{-1} after successfully introducing OEO into films prepared with chitosan and cellulose nanofibrils, while Wu et al. (2014) found that the absorption peaks in this region became stronger in gelatine/chitosan-based films containing 4% OEO. More pronounced peaks were also found at

1,030 cm^{-1}, associated with C−O bonds (Guerrero et al. 2019; Marín-Silva et al. 2019; Sogut and Cakmak 2020; Silva et al. 2024). Additionally, the presence of essential oil in the formulations was denoted by new absorption peaks at 1,370 cm^{-1}, 1,315 cm^{-1}, 1,204 cm^{-1}, ca. 1,105 cm^{-1}, near 1,052 cm^{-1} and in the 850–860 cm^{-1} region. These new peaks are characteristic of OEO; in particular, those at 1,204 cm^{-1} and 1,105 cm^{-1} could be related to carvacrol, which is typically abundant in OEO (Hernández-Nava et al. 2020; El Fawal and Abu-Serie 2022). Slight intensity changes and wavenumber shifts were noticed in these peaks compared to those observed in pure OEO (Online Resource: Supplementary Fig. S1), suggesting interactions between the essential oil and the other compounds present in the formulations (Hernández-Nava et al. 2020). Overlapping of the FTIR spectra of the films containing 1% and 2% OEO was also noticeable. The changes in the patterns of pure OEO and of 2-MCC-OEO-1 and 2-MCC-OEO-2 demonstrate its successful incorporation into the formulations regardless of the concentration of the essential oil.

Solubility and swelling assays

The films containing 1% and 2% OEO exhibited solubility percentages of 16.85 ± 0.85% and 15.74 ± 1.22%, respectively (Fig. 5). Such results correspond to a significant increase in solubility compared to the same type of film without essential oil (2-MCC: 9.27 ± 2.11%; $p < 0.01$). In contrast, the swelling levels of the films were reduced with the incorporation of OEO (Fig. 4). There was a significant decrease ($p < 0.01$) in the water retention capacity of the films from 53.25 ± 5.97% (2-MCC) to 28.22 ± 10.46% (2-MCC-OEO-2). This decrease was even more pronounced in the films with lower essential oil concentration (2-MCC-OEO-1: 16.10 ± 2.28%). No statistically significant differences in OEO concentration were observed for both the solubility and swelling parameters ($p > 0.01$).

On the one hand, these characteristics of the films in the presence of water come from the action of MCC as a filler and its intermolecular interactions with chitosan, forming a compact network that reduces the ability of water molecules to interact with and diffuse through the polymer matrices (Jahed et al. 2017; Franco et al. 2020; Jung et al. 2020; Ponnusamy et al. 2022). On the other hand, the presence of the essential oil changed the solubility of the films, which could be due to interactions with the hydroxyl groups of chitosan (Jahed et al. 2017). Even though the films with OEO were more soluble, the percentages of solubility were still low and statistically inferior ($p < 0.01$) to those obtained for chitosan formulations cross-linked with citric acid and TPP (CHGCA-TPP) previously developed by our group for the same type of application (Silva et al. 2024). This is in agreement with other studies that reported a significant decrease in the solubility of chitosan films after the

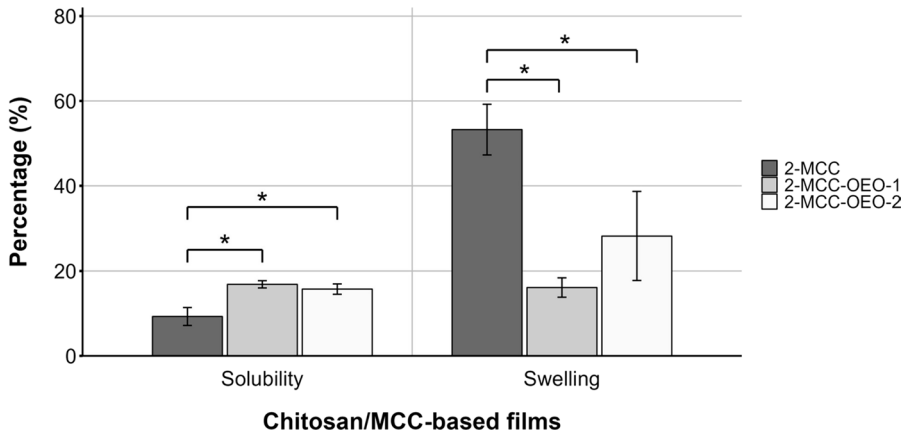

Fig. 5 Percentage of solubility and swelling of chitosan/MCC-based films (2-MCC) and chitosan/MCC-based films reinforced with 1% (2-MCC-OEO-1) and 2% (2-MCC-OEO-2) OEO. The values represent the mean ± standard deviation (n = 3). Statistically significant differences are represented by the symbol * (one-way ANOVA with Tukey B post-hoc test; α = 0.01). MCC: microcrystalline cellulose; OEO: oregano essential oil

incorporation of different essential oils (Ojagh et al. 2010; López-Mata et al. 2013; Jahed et al. 2017).

Wettability assays

The results of the wettability assays, depicted in Fig. 6, indicate that adding 1% or 2% OEO did not significantly reduce the WCAs of the films compared to 2-MCC ($p > 0.01$). The WCA values remained relatively high (> 70°) and close to the water-repellence threshold, and no statistically significant differences were observed with respect to the concentration of the essential oil ($p > 0.01$). Furthermore, the WCAs of all the films slightly increased over time (3 to 15% increase rates) between the beginning and the end of the experiments (Online Resource: Supplementary Fig. S2). Therefore, the low affinity of the films for water was further confirmed by the wettability assays.

Assessment of antimicrobial activity

The antimicrobial activity of the 2-MCC, 2-MCC-OEO-1 and 2-MCC-OEO-2 formulations was evaluated by incubating the sterile solid films with bacterial (*Staphylococcus aureus*, *Bacillus cereus* and *Pseudomonas aeruginosa*) and fungal (*Rhodotorula* spp. and *Penicillium chrysogenum*) strains (Fig. 7).

The growth of *S. aureus* (Fig. 7a) was reduced over time compared to the growth pattern of this strain when inoculated in liquid media without the films (positive control). The reduction in the growth capacity of *S. aureus* was evident after only 3 h of incubation with 2-MCC and this trend remained stable after 24 h. However, only < 1-log reduction in the growth rate of *S. aureus* was achieved at the final time point compared to the bacterial concentration at the beginning of the experiment. When the same strain was incubated with films containing OEO, the inhibition of *S. aureus* was much more pronounced, and no significant differences were found regarding the concentration of OEO ($p > 0.01$). For both concentrations of essential oil, no CFUs were detected within the first 3 h of the experiment.

The growth pattern of *B. cereus* (Fig. 7b) incubated with 2-MCC was similar to that of *S. aureus* and inhibition was observed within the first hours. However, the growth capacity of the strain was recovered over time. Similarly, there was a reduction in bacterial growth capacity during the first hours of incubation with 2-MCC-OEO-1. However, these films had a more prolonged inhibitory effect, which remained constant until the end of the incubation period. The same inhibitory effect was achieved for the films with a higher concentration of essential oil (2%) and no significant differences were recorded regarding the concentration of OEO ($p > 0.01$). It is noteworthy that growth inhibition with 2-MCC-OEO-2 was noticed immediately at the beginning of the experiment and that the concentration of viable cells at the first sampling time point (0 h) was lower

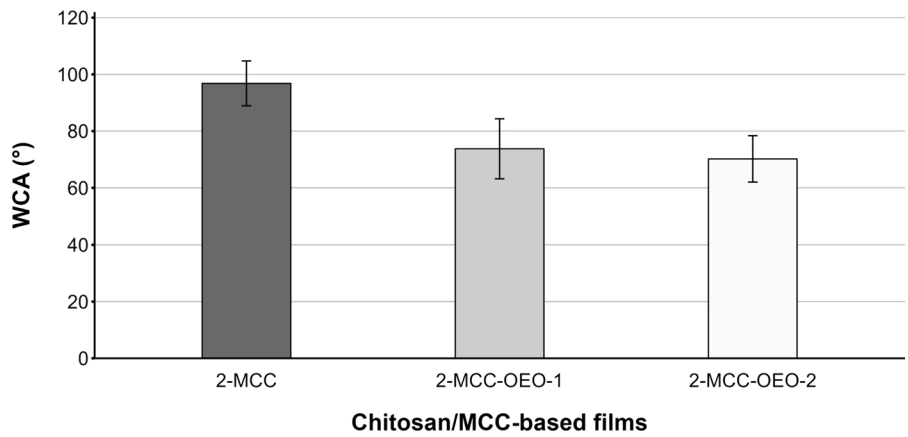

Fig. 6 Water contact angle of chitosan/MCC-based films (2-MCC) and chitosan/MCC-based films reinforced with 1% (2-MCC-OEO-1) and 2% (2-MCC-OEO-2) OEO. The values shown are the mean ± standard deviation (n = 3). No statistically significant differences were found among the films (one-way ANOVA with Tukey B post-hoc test; α = 0.01). MCC: microcrystalline cellulose; OEO: oregano essential oil; WCA: water contact angle

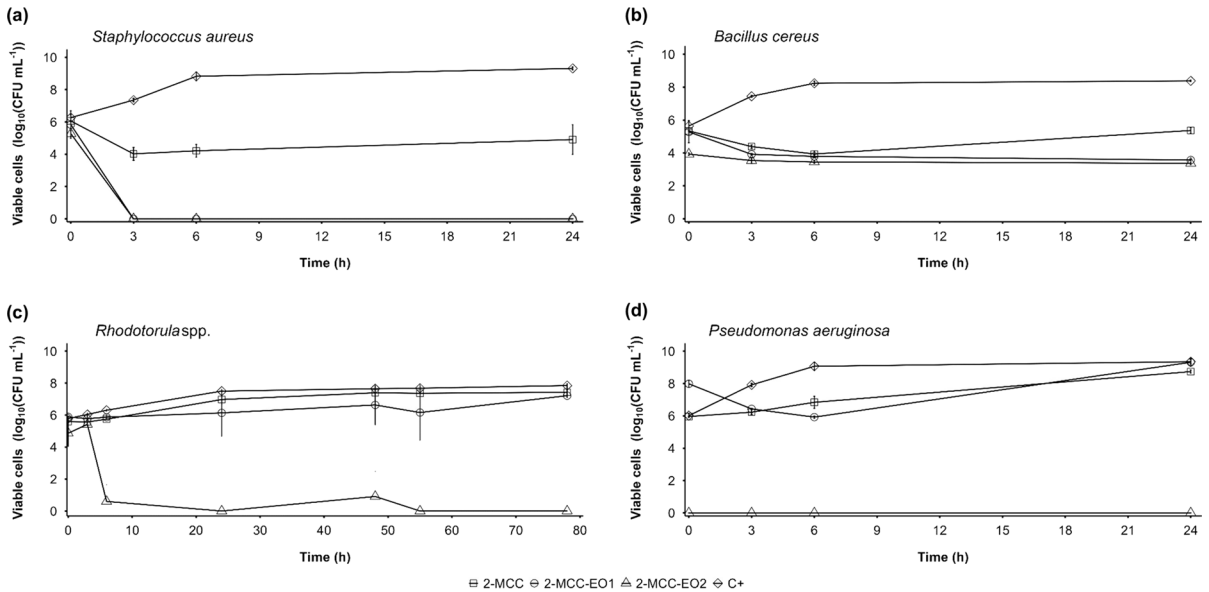

Fig. 7 Concentration of viable cells of **a** *Staphylococcus aureus*, **b** *Bacillus cereus*, **c** *Rhodotorula* spp. and **d** *Pseudomonas aeruginosa* incubated with chitosan/MCC-based films (□ 2-MCC) and chitosan/MCC-based films reinforced with 1% (○ 2-MCC-OEO-1) and 2% (Δ 2-MCC-OEO-2) OEO. The same strains were incubated without films and used as controls (◇). The values represent the mean ± standard deviation (n = 3). MCC: microcrystalline cellulose; OEO: oregano essential oil

(ca. 4 $\log_{10}$ (CFU mL^{-1})) than the initial inoculum of *B. cereus* (ca. 6 $\log_{10}$ (CFU mL^{-1})).

Contrary to what was observed for *S. aureus* and *B. cereus*, 2-MCC failed to inhibit *Rhodotorula* spp. and similar growth patterns were produced when this strain was incubated either with or without the film (Fig. 7c). A comparable behaviour was noted when the *Rhodotorula* spp. cells were incubated with 2-MCC-OEO-1, with an increase in growth of ca. 1 log relative to the concentration of viable cells at the start of the experiment. In contrast, 2-MCC-OEO-2 reduced the concentration of viable *Rhodotorula* spp. cells after only 6 h of incubation. Cell concentration remained low over time, and, at the end of the experiment, complete inhibition of yeast growth was confirmed, with no CFU counts in the PDA plates.

As reported for *Rhodotorula* spp., *Pseudomonas aeruginosa* (Fig. 7d) was not inhibited when incubated with 2-MCC, although a slower growth rate was noticeable in the first hours, which increased over time to reach levels similar to those of the positive control. Likewise, a decrease in bacterial growth was identified in the first hours of incubation with 2-MCC-OEO-1, but the *P. aeruginosa* cell numbers were recovered over time. On the contrary, 2-MCC-OEO-2 was effective in completely inhibiting this strain and no CFUs were recorded during the entire incubation period of *P. aeruginosa* with the film.

The antifungal activity of the films on the growth of *Penicillium chrysogenum* (Table 2) was evaluated by the ability of the fungal spores to germinate in contact with the solid films placed on PDA plates. After 4 days of incubation, colonies of ca. 22 mm

Table 2 Growth inhibition of *Penicillium chrysogenum* after incubation with chitosan/MCC-based films (2-MCC) and chitosan/MCC-based films with 1% (2-MCC-OEO-1) and 2% (2-MCC-OEO-2) OEO

Sample	Fungal growth inhibition (%)
2-MCC	100.00 ± 0.00^{a}
2-MCC-OEO-1	100.00 ± 0.00^{a}
2-MCC-OEO-2	59.66 ± 8.11^{b}

The concentrations of chitosan, acetic acid and glycerol were fixed at 1% for all formulations. CA: citric acid; CNC: cellulose nanocrystals; MCC: microcrystalline cellulose; OEO: oregano essential oil; TPP: sodium tripolyphosphate

in diameter were observed in the positive controls. No growth of *P. chrysogenum* was detected on the 2-MCC and 2-MCC-OEO-1 films, and complete inhibition of fungal growth (100%) was recorded when compared to inoculation on filter paper discs (positive control). However, 2-MCC-OEO-2 induced ca. 60% inhibition ($p < 0.01$) and small fungal colonies were present on the films at the end of the incubation period.

The incubation of 2-MCC-OEO-1 and 2-MCC-OEO-2 films with bacterial and fungal strains partially or completely inhibited their growth capacity, depending on the strain under test. It is presumed that the immobilisation of chitosan molecules by cross-linking interactions with MCC reduced the number of free amino groups able to interact with the cell surfaces of some of the microorganisms and induce cell lysis (Wu et al. 2014). The presence of the OEO, therefore, seems to be necessary to induce a greater inhibitory effect in some strains. For example, Chen et al. (2020) reported a significant improvement in the antibacterial properties of chitosan films after the addition of OEO and demonstrated good inhibitory properties against *Escherichia coli* and *Listeria monocytogenes*. The authors also suggested an optimum OEO concentration of 2% to ensure high antibacterial activity (Chen et al. 2020). Similarly, J. Wu et al. (2014) demonstrated that, even though gelatine-chitosan-based films had no antibacterial activity against several microorganisms, the incorporation of OEO into the films at concentrations higher than 1% resulted in inhibition of bacterial growth.

The germination of *Penicillium chrysogenum* spores on 2-MCC and 2-MCC-OEO-1 films was completely suppressed, but small fungal colonies were still able to grow on 2-MCC-OEO-2 films. The synergistic or additive effects of chitosan and essential oils against fungal strains have been reviewed in the literature (Yuan et al. 2016; Grande-Tovar et al. 2018). For example, Mohammadi et al. (2016) concluded that the combination of chitosan and essential oils was more effective in reducing *Phytophthora drechsleri* mycelial growth than either pure essential oils or chitosan. However, in the study reported herein, increasing the concentration of OEO seemed to have had an antagonistic effect and reduced the inhibition rate of fungal growth. Nevertheless, 2-MCC-OEO-2 still induced a substantial inhibition of *Penicillium chrysogenum* of ca. 60%. Even though the comparison of antimicrobial results with those reported in the literature is subjective due to differences in methodology and the variety and composition of essential oils, still some studies have reported the antifungal activity of chitosan-based films containing different types of essential oils. Recently, Hossain et al. (2019) observed significant antifungal activity of chitosan films reinforced with CNCs and several essential oil nanoemulsions (including oregano) against *P. chrysogenum* and *Aspergillus* strains by vapour phase assays, reporting growth reductions of 51–77%. Similar conclusions were reached by Guo et al. (2022), who demonstrated that OEO added to chitosan films had antifungal properties against *Alternaria alternata*.

Overall, OEO was successfully incorporated into the formulation. The films with essential oil remained poorly soluble, with low percentages of swelling and without significantly affecting their structure after immersion in water. The presence of the essential oil, regardless of its concentration, did not affect significantly the WCAs of the films compared to those with only MCC, and the values remained high and near the water-repellence threshold. The 2-MCC films without essential oil reduced the concentration of viable *S. aureus* cells by the end of the assays, but not of *B. cereus*, *Rhodotorula* spp. or *P. aeruginosa*. However, adding OEO contributed to a better antimicrobial performance of the formulations, mainly when used at a concentration of 2%. Complete growth inhibition was achieved for *S. aureus* (regardless of the concentration of essential oil), as well as for *Rhodotorula* spp. and *P. aeruginosa* when incubated with the formulations with 2% OEO, while the concentration of viable *B. cereus* cells was partially reduced. Additionally, although films with OEO at 2% did not completely inhibit spore germination and fungal growth, it caused a significant reduction in *Penicillium chrysogenum* development and proliferation. These results constitute an improvement in the antimicrobial action of the CHGCA-TPP formulations previously reported by our group in another study (Silva et al. 2024). Compared to CHGCA-TPP films (Silva et al. 2024), the chitosan matrices reinforced with MCC and OEO proved to be more effective at preventing the growth of the microorganisms tested. Even though CHGCA-TPP significantly reduced the growth of most strains, complete inhibition was not reached. In contrast, 2-MCC-OEO-2 not only suppressed the growth of

S. aureus and *Rhodotorula* spp. and sustained *B. cereus* and *P. chrysogenum* at low concentrations, but also had an inhibitory effect on the Gram-negative *Pseudomonas aeruginosa*, as opposed to that observed for CHGCA-TPP, which neither prevented nor significantly slowed its growth.

Considering the results reported above, 2-MCC-OEO-2 exhibited similar solubility, swelling and wettability to 2-MCC-OEO-1, but better antimicrobial activity against most of the microbial strains tested. Consequently, the 2-MCC-OEO-2 formulation was applied to granite, marble and limestone and the stones were characterised after polymerisation of the coating.

Characterisation of stone samples coated with 2-MCC-OEO-2

Scanning electron microscopy analysis

Morphological observations by scanning electron microscopy (SEM) demonstrated the deposition and polymerisation of the coating on the surfaces of granite, limestone and marble (Fig. 8). Fragments of the coating were discernible as dark patches on the stones, which contrasted with the lighter areas of the uncoated stones. The analysis revealed that the coating was not uniformly distributed and that the uncoated areas tended to be at the edges of the samples, with the coating mostly present in the centre. The uneven distribution of the coating could be related to the absorption of part of the solution by the stones' pores and the method of application using a micropipette tip to spread the liquid (Silva et al. 2024).

Fourier transformed infrared spectroscopy analysis

FTIR analysis showed similar absorption patterns between the 2-MCC-OEO-2 film (Fig. 4a) and the coated granite and marble samples (Fig. 4b). On the contrary, the FTIR spectrum of coated limestone (Fig. 4b) was considerably different from that of the 2-MCC-OEO-2 film, with short peaks being detected mainly at 2,530 cm^{-1}, 2,160 cm^{-1}, 2,040–1,970 cm^{-1} and 1,055 cm^{-1}. This may have occurred because the analysis was possibly carried out in areas with poor coating coverage and the 2-MCC-OEO-2 formulation was not detected on the surface of the limestone sample.

Wettability assays

The WCA values of the coated stones were higher than 70° and close to the threshold of water-repellence (Table 3). The granite samples had the lowest mean WCA values ($73.35 \pm 12.20°$), which was consistent with that of the 2-MCC-OEO-2 film polymerised in Petri dishes ($70.20 \pm 8.18°$). The mean WCAs of limestone and marble were slightly higher, with values of $88.26 \pm 3.12°$ and $92.88 \pm 9.54°$, respectively.

The WCAs of the coated stones were significantly higher than those reported in a previous study by our group for uncoated stones of the same type ($p < 0.05$; Silva et al. 2024). That study showed that the uncoated surfaces of granite, limestone and marble had low WCAs ($29.83 \pm 15.68°$, $41.94 \pm 2.64°$ and $57.18 \pm 2.36°$, respectively). An increase of 146% in the WCAs values was observed in granite coated with 2-MCC-OEO-2 compared to uncoated samples, while a 110% and 62% increase was observed for coated limestone and marble, respectively.

In a previous study, the wettability of granite and limestone decreased after coating with a chitosan formulation containing citric acid and TPP (CHGCA-TPP-a), with WCAs reaching ca. 60–65° (Silva et al. 2024). However, in the current study, the increase in WCAs after coating with 2-MCC-EO-2 was more pronounced. Marble and limestone coated with 2-MCC-OEO-2 showed significantly higher WCAs compared to the same stones coated with CHGCA-TPP-a ($p < 0.01$), while no differences were found in granite samples regarding the type of coating ($p > 0.01$).

Nevertheless, the variability in the WCAs depending on the type of stone may be related to differences in the porosity of each substrate, as different pore sizes can influence the penetration degree of the coating. Further research is necessary to determine the porosity and permeability properties of the stone samples and evaluate the degree of absorption of the coating by the stone pores.

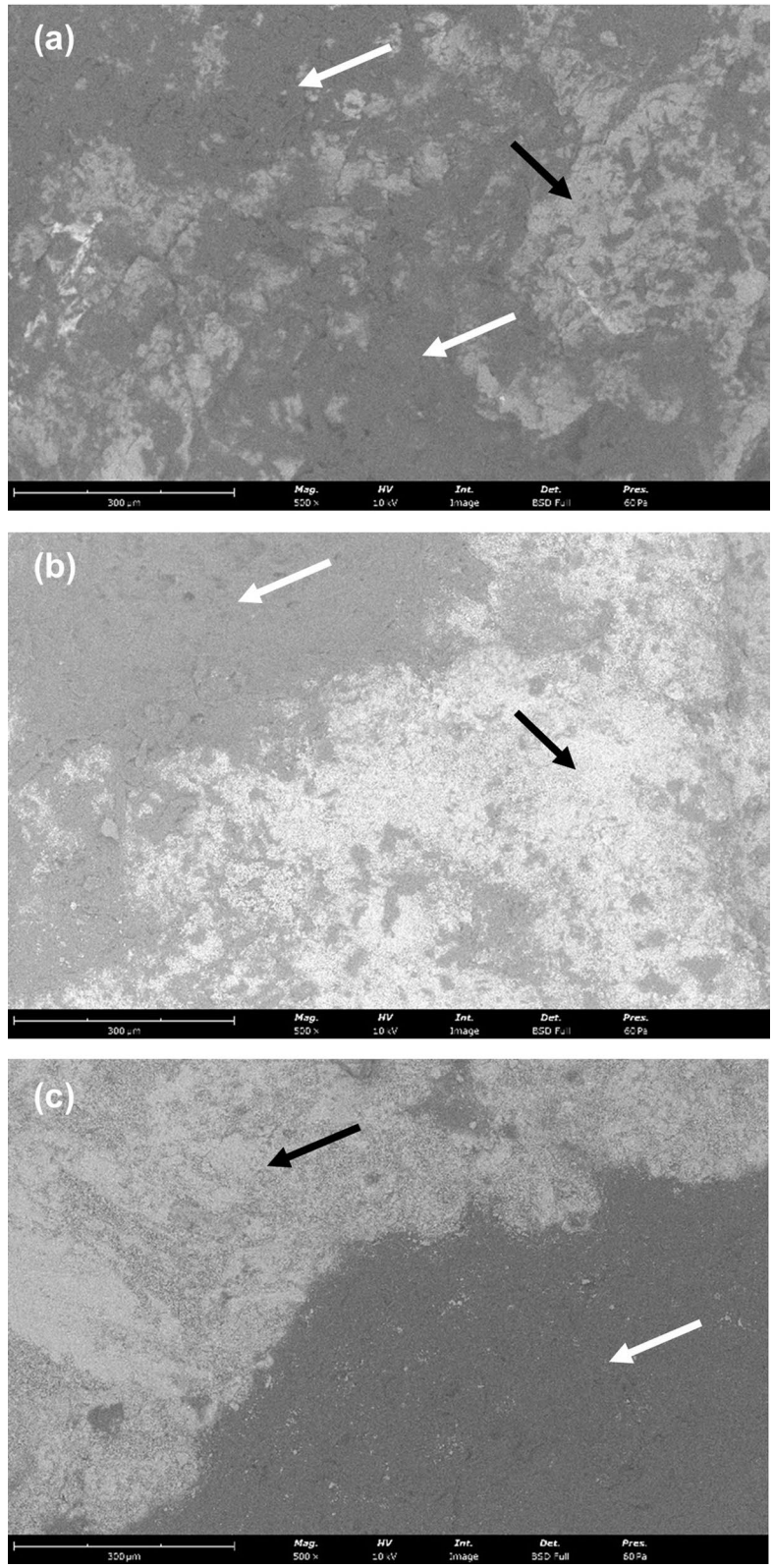

Fig. 8 Scanning electron microscopy images of **a** granite, **b** limestone and **c** marble coated with 2-MCC-OEO-2. The white arrows point to fragments of the 2-MCC-OEO-2 coating and the black arrows show areas of uncoated stone. MCC: microcrystalline cellulose; OEO: oregano essential oil

Table 3 Water contact angle of granite, limestone and marble, uncoated and coated with 2-MCC-OEO-2

WCA (°)		
Stone type	Uncoated*	Coated
Granite	29.83 ± 15.68^{a}	73.35 ± 12.20^{b}
Limestone	41.94 ± 2.64^{a}	88.26 ± 3.12^{b}
Marble	57.18 ± 2.36^{a}	92.88 ± 9.54^{b}

*The WCA values of the uncoated samples are those reported by Silva and co-authors (2024) and were used here for comparison with the 2-MCC-OEO-2-coated samples. The values represent the mean ± standard deviation (n = 3). In each row, different letters represent statistically significant differences between uncoated and coated samples (independent samples ttests; α = 0.05). MCC: microcrystalline cellulose; OEO: oregano essential oil; WCA: water contact angle

Table 4 Colour differences (ΔE^*_{ab}) of stone samples before and after coating with 2-MCC-OEO-2

Stone type	Micropipette	Brush
Granite	5.89 ± 2.25^{a}	1.01 ± 0.26^{a}
Limestone	0.28 ± 0.02^{a}	1.96 ± 0.53^{a}
Marble	8.05 ± 0.13^{a}	0.65 ± 0.46^{b}

The 2-MCC-OEO-2 formulation was spread over the upper surfaces of the stones using micropipette tips or a brush. The values represent the mean ± standard deviation (n = 3). In the same row, different letters represent statistically significant differences between the mode of application of the coating (independent samples ttests; α = 0.01). MCC: microcrystalline cellulose; OEO: oregano essential oil

Colourimetric assays

The chromatic changes (ΔE^*_{ab}) before and after the application of the coating and its polymerisation on the stone samples are reported in Table 4. Spreading the coating-forming solution over the upper surfaces of the slabs with the micropipette tips produced ΔE^*_{ab} values of ca. 6 and 8 on granite and marble, respectively. However, when the same solution was spread with a brush, the colour differences were much lower (ca. 1; Table 4). The opposite was true for limestone, where brush application resulted in a greater colour change on its surface than deposition and spreading of the coating-forming solution with a micropipette; it is not clear why this occurred, but the differences in the method of application were not significant ($p > 0.01$). Nevertheless, the ΔE^*_{ab} values remained below 2 for all stone types when a brush was used.

The values registered when using either a micropipette or a brush are within the range considered acceptable by some authors for the colour changes produced on porous materials. García and Malaga (2012) and Ortiz et al. (2013) have suggested that ΔE^*_{ab} values between 5 and 10 are acceptable for porous materials despite such colour differences being perceived with the naked eye. However, other studies suggest an $\Delta E^*_{ab} < 5$, as such values correspond to chromatic differences that are not perceptible to humans (Sasso et al. 2016; Goffredo et al. 2017; Becerra et al. 2019; Tortora et al. 2020). In the study herein described, limestone had a very low ΔE^*_{ab} value, while granite and marble had $\Delta E^*_{ab} > 5$ when the coating was directly deposited with a micropipette. However, $\Delta E^*_{ab} < 2$ were obtained for all stone types when 2-MCC-OEO-2 was applied with a brush, mimicking an on-site application on immovable stone artwork. Therefore, the coating should not introduce visible colour changes to stone heritage. However, it should be noted that part of the formulations was retained in the brush fibres and future studies should clarify the amount of coating lost with this method of application and its influence on the colour of the stone samples, as well as possibly considering other ways of applying the coating on these types of surfaces (e. g. spraying). Additionally, more research is necessary to ascertain the presence of the coating on the surfaces. Since a uniform distribution of the coating was not achieved, as observed by SEM, it is possible that the absence of visible colour changes is related to the absorption of substantial portions of the formulation and incomplete coverage of the surfaces of the stones (Silva et al. 2024).

In summary, the application of 2-MCC-OEO-2 to granite, marble and limestone formed a protective but irregular layer on the stones' surfaces, possibly due to uneven distribution of the coating or absorption and polymerisation of some of the solution into the stone pores. The wettability of the stones' surfaces was reduced, while not becoming completely water-repellent. 2-MCC-OEO-2 changed the aesthetic appearance of granite and marble only when the solution was spread with a micropipette, but no colour alterations were visible when a brush was used.

The use of chitosan and cellulose crystals for heritage conservation is still very limited and the

development of coatings based on these polymers for outdoor sculpture applications is innovative and challenging. The work presented in this article is a contribution to the advancement of knowledge in this field and to open up new possibilities to establish more sustainable programmed preventive strategies. However, some limitations were found that should be further investigated. Specifically, aspects relating to the most suitable method for applying the coating and the quantity required to achieve a more homogeneous coating of the surfaces need to be studied in more detail, as well as perform further colourimetric studies to confirm the absence of aesthetic changes on the surfaces after coating. Properties such as porosity, water capillarity and surface roughness of the stone samples could not be characterised in this study and should be investigated in the future. Such properties may influence the adhesiveness of the coatings to the lithic materials, their absorption degree and distribution patterns at endolithic and epilithic levels, and how they alter the intrinsic properties of each lithotype. Likewise, assays involving the exposure of coated stones to ageing factors, as well as to natural environmental conditions and biological contamination, should be carried out over an extended period of time to evaluate (and possibly improve) the durability and efficacy of the coating in outdoor locations before testing on stone sculptures. Nonetheless, the chitosan-based formulations that were tested, especially when reinforced with MCC and OEO, constitute a potential foundation for the development and optimisation of new, low-toxicity antimicrobial coatings towards more sustainable preventive conservation strategies of stone heritage.

Conclusions

Chitosan formulations with CNC and MCC were developed as a preventive treatment for stone artworks against microbial contamination. The formulation containing 2% MCC was selected for further analysis and supplemented with OEO (at 1% and 2%), exhibiting low solubility, swelling and wettability when polymerised in film form. These films showed good antimicrobial capacity against microorganisms that can be found in stone microbiomes and could be involved in deterioration processes in monuments and sculptures. The application of the formulation with 2% OEO to granite, marble and limestone formed a protective, yet irregular coating on the surfaces, and decreased the wettability of the stones without producing relevant changes in their aesthetic appearance when it was applied with a brush. Although further studies are encouraged to improve and optimise the formulations, the study presented herein is a step towards developing biodegradable antimicrobial coatings with low toxicity for cultural heritage applications. In particular, chitosan-MCC-OEO coatings have the potential to be used as protective layers for stone heritage, including outdoor sculptures, towards more sustainable strategies for its preservation against biodeterioration.

Acknowledgments The authors are grateful to FCT and FSE for the financial support. The authors would also like to thank the scientific collaboration under the FCT projects UID/Multi/50016/2013, UID/Multi/50016/2019 and UIDB/50016/2020. The authors acknowledge Sérgio Sousa for his assistance with SEM analysis.

Author contributions N.C.S.: Data curation, Formal analysis, Funding acquisition, Investigation, Methodology, Visualisation, Writing-original draft, Writing-review and editing. A.R.M.: Conceptualisation, Funding acquisition, Project administration, Supervision, Writing-review and editing. M.P.: Conceptualisation, Funding acquisition, Project administration, Resources, Supervision, Writing-review and editing. P.R.M.: Conceptualisation, Funding acquisition, Methodology, Project administration, Resources, Supervision, Writing-review and editing.

Funding Open access funding provided by FCT|FCCN (b-on). This work was supported by FCT – Fundação para a Ciência e a Tecnologia through projects BIONANOSCULP (grant number PTDC/EPH-PAT/6281/2014), UID/Multi/50016/2013, UID/Multi/50016/2019 and UIDB/50016/2020. Author Nádia C. Silva received financial support from FCT and FSE – Fundo Social Europeu through Programa Operacional Regional Norte (grant number SFRH/BD/138935/2018).

Data availability Data can be made available on request.

Declarations

Competing interests The authors declare no competing interests.

References

Abdul Khalil HPS, Chong EWN, Owolabi FAT et al (2019) Enhancement of basic properties of polysaccharide-based composites with organic and inorganic fillers: a review. J Appl Polym Sci 136:47251. https://doi.org/10.1002/app.47251

Bagheri M, Younesi H, Hajati S, Borghei SM (2015) Application of chitosan-citric acid nanoparticles for removal of chromium (VI). Int J Biol Macromol 80:431–444. https://doi.org/10.1016/j.ijbiomac.2015.07.022

Bakshi PS, Selvakumar D, Kadirvelu K, Kumar NS (2020) Chitosan as an environment friendly biomaterial – a review on recent modifications and applications. Int J Biol Macromol 150:1072–1083. https://doi.org/10.1016/j.ijbiomac.2019.10.113

Becerra J, Mateo M, Ortiz P et al (2019) Evaluation of the applicability of nano-biocide treatments on limestones used in cultural heritage. J Cult Herit 38:126–135. https://doi.org/10.1016/j.culher.2019.02.010

Chen S, Wu M, Wang C et al (2020) Developed chitosan/oregano essential oil biocomposite packaging film enhanced by cellulose nanofibril. Polymers 12:1780. https://doi.org/10.3390/polym12081780

Dakal TC, Cameotra SS (2012) Microbially induced deterioration of architectural heritages: routes and mechanisms involved. Environ Sci Eur 24:1–13. https://doi.org/10.1186/2190-4715-24-36

El Fawal G, Abu-Serie MM (2022) Bioactive properties of nanofibers based on poly(vinylidene fluoride) loaded with oregano essential oil: fabrication, characterization and biological evaluation. J Drug Deliv Sci Technol 69:103133. https://doi.org/10.1016/j.jddst.2022.103133

Franco TS, Amezcua RMJ, Rodrìguez AV et al (2020) Carboxymethyl and nanofibrillated cellulose as additives on the preparation of chitosan biocomposites: their influence over films characteristics. J Polym Environ 28:676–688. https://doi.org/10.1007/s10924-019-01639-0

Gadd GM (2017) Geomicrobiology of the built environment. Nat Microbiol 2:16275. https://doi.org/10.1038/nmicrobiol.2016.275

García O, Malaga K (2012) Definition of the procedure to determine the suitability and durability of an anti-graffiti product for application on cultural heritage porous materials. J Cult Herit 13:77–82. https://doi.org/10.1016/j.culher.2011.07.004

Gierszewska M, Ostrowska-Czubenko J (2016) Chitosan-based membranes with different ionic crosslinking density for pharmaceutical and industrial applications. Carbohydr Polym 153:501–511. https://doi.org/10.1016/j.carbpol.2016.07.126

Goffredo GB, Accoroni S, Totti C et al (2017) Titanium dioxide based nanotreatments to inhibit microalgal fouling on building stone surfaces. Build Environ 112:209–222. https://doi.org/10.1016/j.buildenv.2016.11.034

Grande-Tovar CD, Chaves-Lopez C, Serio A et al (2018) Chitosan coatings enriched with essential oils: effects on fungi involve in fruit decay and mechanisms of action. Trends Food Sci Technol 78:61–71. https://doi.org/10.1016/j.tifs.2018.05.019

Guerrero P, Muxika A, Zarandona I, de la Caba K (2019) Crosslinking of chitosan films processed by compression molding. Carbohydr Polym 206:820–826. https://doi.org/10.1016/j.carbpol.2018.11.064

Guo S, Li T, Chen M et al (2022) Sustainable and effective chitosan-based edible films incorporated with OEO nanoemulsion against apricots' black spot. Food Control 138:108965. https://doi.org/10.1016/j.foodcont.2022.108965

Haghighi H, Licciardello F, Fava P et al (2020) Recent advances on chitosan-based films for sustainable food packaging applications. Food Packag Shelf Life 26:100551. https://doi.org/10.1016/j.fpsl.2020.100551

Hernández-Nava R, López-Malo A, Palou E et al (2020) Encapsulation of oregano essential oil (Origanum vulgare) by complex coacervation between gelatin and chia mucilage and its properties after spray drying. Food Hydrocoll 109:106077. https://doi.org/10.1016/j.foodhyd.2020.106077

Herrera LK, Videla HA (2009) Surface analysis and materials characterization for the study of biodeterioration and weathering effects on cultural property. Int Biodeterior Biodegrad 63:813–822. https://doi.org/10.1016/j.ibiod.2009.05.002

Hossain F, Follett P, Salmieri S et al (2019) Antifungal activities of combined treatments of irradiation and essential oils (EOs) encapsulated chitosan nanocomposite films in in vitro and in situ conditions. Int J Food Microbiol 295:33–40. https://doi.org/10.1016/j.ijfoodmicro.2019.02.009

Jahed E, Khaledabad MA, Bari MR, Almasi H (2017) Effect of cellulose and lignocellulose nanofibers on the properties of Origanum vulgare ssp. gracile essential oil-loaded chitosan films. React Funct Polym 117:70–80. https://doi.org/10.1016/j.reactfunctpolym.2017.06.008

Jung J, Deng Z, Zhao Y (2020) A review of cellulose nanomaterials incorporated fruit coatings with improved barrier property and stability: Principles and applications. J Food Process Eng 43:e13344. https://doi.org/10.1111/jfpe.13344

Kakakhel MA, Wu F, Gu J-D et al (2019) Controlling biodeterioration of cultural heritage objects with biocides: a review. Int Biodeterior Biodegrad 143:104721. https://doi.org/10.1016/j.ibiod.2019.104721

Kaplan Z, Böke H, Sofuoglu A, İpekoğlu B (2019) Long term stability of biodegradable polymers on building limestone. Prog Org Coatings 131:378–388. https://doi.org/10.1016/j.porgcoat.2019.03.004

Khallaf MK, El-Midany AA, El-Mofty SE (2011) Influence of acrylic coatings on the interfacial, physical, and

mechanical properties of stone-based monuments. Prog Org Coatings 72:592–598. https://doi.org/10.1016/j.porgcoat.2011.06.021

Kumar S, Mukherjee A, Dutta J (2020) Chitosan based nanocomposite films and coatings: emerging antimicrobial food packaging alternatives. Trends Food Sci Technol 97:196–209. https://doi.org/10.1016/j.tifs.2020.01.002

Liu Y, Shen X, Zhou H et al (2016) Chemical modification of chitosan film via surface grafting of citric acid molecular to promote the biomineralization. Appl Surf Sci 370:270–278. https://doi.org/10.1016/j.apsusc.2016.02.124

Liu X, Koestler RJ, Warscheid T et al (2020) Microbial deterioration and sustainable conservation of stone monuments and buildings. Nat Sustain 3:991–1004. https://doi.org/10.1038/s41893-020-00602-5

López-Mata MA, Ruiz-Cruz S, Silva-Beltrán NP et al (2013) Physicochemical, antimicrobial and antioxidant properties of chitosan films incorporated with carvacrol. Molecules 18:13735–13753. https://doi.org/10.3390/molecules181113735

Lusiana RA, Protoningtyas WP, Wijaya AR, Siswanta D et al (2017) Chitosan-tripoly phosphate (CS-TPP) synthesis through cross-linking process: the effect of concentration towards membrane mechanical characteristic and urea permeation. Orient J Chem 33:2913–2919. https://doi.org/10.13005/ojc/330626

Marín-Silva DA, Rivero S, Pinotti A (2019) Chitosan-based nanocomposite matrices: development and characterization. Int J Biol Macromol 123:189–200. https://doi.org/10.1016/j.ijbiomac.2018.11.035

Mathew GM, Mathew DC, Sukumaran RK et al (2020) Sustainable and eco-friendly strategies for shrimp shell valorization. Environ Pollut 267:115656. https://doi.org/10.1016/j.envpol.2020.115656

Mohammadi A, Hashemi M, Hosseini SM (2016) Integration between chitosan and Zataria multiflora or Cinnamomum zeylanicum essential oil for controlling Phytophthora drechsleri, the causal agent of cucumber fruit rot. LWT - Food Sci Technol 65:349–356. https://doi.org/10.1016/j.lwt.2015.08.015

Negi A, Sarethy IP (2019) Microbial biodeterioration of cultural heritage: events, colonization, and analyses. Microb Ecol 78:1014–1029. https://doi.org/10.1007/s00248-019-01366-y

Ocak Y, Sofuoglu A, Tihminlioglu F, Böke H (2009) Protection of marble surfaces by using biodegradable polymers as coating agent. Prog Org Coatings 66:213–220. https://doi.org/10.1016/j.porgcoat.2009.07.007

Ojagh SM, Rezaei M, Razavi SH, Hosseini SMH (2010) Development and evaluation of a novel biodegradable film made from chitosan and cinnamon essential oil with low affinity toward water. Food Chem 122:161–166. https://doi.org/10.1016/j.foodchem.2010.02.033

Ortiz P, Antúnez V, Ortiz R et al (2013) Comparative study of pulsed laser cleaning applied to weathered marble surfaces. Appl Surf Sci 283:193–201. https://doi.org/10.1016/j.apsusc.2013.06.081

Pavinatto A, de Mattos AV, A, Malpass ACG, et al (2020) Coating with chitosan-based edible films for mechanical/biological protection of strawberries. Int J Biol Macromol 151:1004–1011. https://doi.org/10.1016/j.ijbiomac.2019.11.076

Ponnusamy PG, Sundaram J, Mani S (2022) Preparation and characterization of citric acid crosslinked chitosan-cellulose nanofibrils composite films for packaging applications. J Appl Polym Sci 139:e52017. https://doi.org/10.1002/app.52017

Ranalli G, Zanardini E, Sorlini C, Moselio S (2009) Biodeterioration - including cultural heritage. Encycl Microbiol. https://doi.org/10.1016/B978-012373944-5.00132-2

Rinaudo M (2006) Chitin and chitosan: properties and applications. Prog Polym Sci 31:603–632. https://doi.org/10.1016/j.progpolymsci.2006.06.001

Rudic O, Ranogajec J, Vulic T et al (2014) Photo-induced properties of TiO_2/ZnAl layered double hydroxide coating onto porous mineral substrates. Ceram Int 40:9445–9455. https://doi.org/10.1016/j.ceramint.2014.02.017

Sacco P, Borgogna M, Travan A et al (2014) Polysaccharide-based networks from homogeneous chitosan-tripolyphosphate hydrogels: synthesis and characterization. Biomacromol 15:3396–3405. https://doi.org/10.1021/bm500909n

Sasso S, Miller AZ, Rogerio-Candelera MA et al (2016) Potential of natural biocides for biocontrolling phototrophic colonization on limestone. Int Biodeterior Biodegrad 107:102–110. https://doi.org/10.1016/j.ibiod.2015.11.017

Sdiri A, Higashi T, Hatta T et al (2010) Mineralogical and spectroscopic characterization, and potential environmental use of limestone from the Abiod formation, Tunisia. Environ Earth Sci 61:1275–1287. https://doi.org/10.1007/s12665-010-0450-5

Sierra-Fernandez A, Gomez-Villalba LS, Rabanal ME, Fort R (2017) New nanomaterials for applications in conservation and restoration of stony materials: a review. Mater Construcción 67:e107. https://doi.org/10.3989/mc.2017.07616

Silva NC, Castro D, Neto C et al (2024) Antimicrobial chitosan/TPP-based coatings for the prevention of biodeterioration of outdoor stone sculptures. Prog Org Coatings 189:108246. https://doi.org/10.1016/j.porgcoat.2024.108246

Sogut E, Cakmak H (2020) Utilization of carrot (Daucus carota L.) fiber as a filler for chitosan based films. Food Hydrocoll 106:105861. https://doi.org/10.1016/j.foodhyd.2020.105861

Tomaz AF, de Carvalho SMS, Barbosa RC et al (2018) Ionically crosslinked chitosan membranes used as drug carriers for cancer therapy application. Materials 11:2051. https://doi.org/10.3390/ma11102051

Tortora M, Chiarini M, Spreti N, Casieri C (2020) 1H-NMR-relaxation and colorimetry for evaluating nanopolymeric dispersions as stone protective coatings. J Cult Herit 44:204–210. https://doi.org/10.1016/j.culher.2019.12.014

Wu J, Ge S, Liu H et al (2014) Properties and antimicrobial activity of silver carp (Hypophthalmichthys molitrix) skin gelatin-chitosan films incorporated with oregano essential oil for fish preservation. Food Packag Shelf Life 2:7–16. https://doi.org/10.1016/j.fpsl.2014.04.004

Wu C, Sun J, Lu Y et al (2019a) In situ self-assembly chitosan/ε-polylysine bionanocomposite film with enhanced antimicrobial properties for food packaging. Int J Biol Macromol 132:385–392. https://doi.org/10.1016/j.ijbiomac.2019.03.133

Wu H, Lei Y, Lu J et al (2019b) Effect of citric acid induced crosslinking on the structure and properties of potato starch/chitosan composite films. Food Hydrocoll 97:105208. https://doi.org/10.1016/j.foodhyd.2019.105208

Yuan G, Chen X, Li D (2016) Chitosan films and coatings containing essential oils: the antioxidant and antimicrobial activity, and application in food systems. Food Res Int 89:117–128. https://doi.org/10.1016/j.foodres.2016.10.004